Phase separation of self-propelled ballistic particles

Isaac R. Bruss[1] and Sharon C. Glotzer[1,2,3,*]
[1]*Chemical Engineering, University of Michigan, Ann Arbor, Michigan 48109, USA*
[2]*Materials Science & Engineering, University of Michigan, Ann Arbor, Michigan 48109, USA*
[3]*Biointerfaces Institute, University of Michigan, Ann Arbor, Michigan 48109, USA*

(Received 3 December 2017; published 19 April 2018)

Self-propelled particles phase-separate into coexisting dense and dilute regions above a critical density. The statistical nature of their stochastic motion lends itself to various theories that predict the onset of phase separation. However, these theories are ill-equipped to describe such behavior when noise becomes negligible. To overcome this limitation, we present a predictive model that relies on two density-dependent timescales: τ_F, the mean time particles spend between collisions; and τ_C, the mean lifetime of a collision. We show that only when $\tau_F < \tau_C$ do collisions last long enough to develop a growing cluster and initiate phase separation. Using both analytical calculations and active particle simulations, we measure these timescales and determine the critical density for phase separation in both two and three dimensions.

DOI: 10.1103/PhysRevE.97.042609

Statistical physics extracts order from randomness by describing the average behavior of noisy systems. Such noise is prevalent in active matter [1,2], where individual particles generate their own motion by consuming energy from their environment, whether it be from chemical reactions [3–5], vibrations [6,7], light [8], or magnetic fields [9,10]. However, such active systems fall outside the realm of equilibrium statistical physics because, although they may be at steady state, they are inherently nonequilibrium and do not obey detailed balance [11].

Despite these challenges, emergent behaviors are still observed in active matter systems, such as their ability to phase-separate. In particular, active Brownian particles (ABPs), an idealized system of self-propelled hard particles, each with a rotationally diffusing direction of motion [12], have been found to phase-separate into dense and dilute phases [13,14]. This robust behavior has also been found for both two and three dimensions [15], as well as for rodlike [16–18] and shaped particles [19,20], attractive particles [21,22], contact-triggered active particles [23], and mixtures of ABPs with passive particles [24,25].

Two prevailing theories describe motility-induced phase separation (MIPS) for ABPs. One is a kinetic theory that balances the density-dependent inward flux of particles into the dense phase, with a diffusion-dependent outward flux [14,26]. The other is a continuum mean-field theory that attributes phase separation to the reduction in a particle's effective speed by an increasing local density [27–29]. Critical to both of their formulations is the noise involved in the rotational diffusion of the particles. Given a rotational diffusion constant of D_R, the persistence length, ℓ_P, of an active particle moving with a velocity v_0 is v_0/D_R. For the kinetic theory, the rotational diffusion regulates the rate at which boundary particles become unblocked and escape the dense phase. This balance leads to the incorrect prediction in the limit of $\ell_P \to \infty$ of a critical density for phase separation of $\phi_{\text{crit}} = 0$ [14]. However, previous simulations at or approaching this ballistic regime show a nonzero critical density for MIPS (via spinodal decomposition) of $0.25 \gtrsim \phi_{\text{crit}} \gtrsim 0.35$ in two dimensions [28,30–32]. The range of reported densities is likely due to a small system size, with higher ϕ_{crit} being measured for numbers of particles less than 10 000 [33]. Also, these results are for simulations where translational diffusion is zero, which approximates the behavior of run-and-tumble bacteria [12,34]. When translational diffusion is proportional to D_R, $\phi_{\text{crit}} \approx 0.4$ [13,27]. Finally, like the kinetic theory, the continuum theory of MIPS is only meaningful when noise is present for finite ℓ_P, because the effective pressure diverges when $D_R = 0$ [28,31]. And while results for large ℓ_P can still be extracted, numerical fitting parameters are required [31].

Although these two theories explain MIPS in their respective regimes, and can be used to extract other important properties such as cluster fraction and growth rates, there exists a gap in the understanding of MIPS when rotational noise is absent (or, at minimum, when ℓ_P is much greater than a particle's diameter). Examples of such ballistic-regime active matter systems are straight-swimming bacteria that do not tumble due to mutations [35] or hydrodynamic suppression [36], and vibrated polar disks [7]. Here we present a model of MIPS that is independent of rotational noise and sets a lower bound on the critical density required for phase separation. Although a system with zero noise is not strictly ergodic for a finite number of particles, we argue that this detail is irrelevant for phase separation because the initial stages of spinodal decomposition happen on a finite length scale where particle collisions can be considered ergodic.

We demonstrate that the MIPS of ABP systems is dependent on the relation between two density-dependent timescales [shown schematically in Fig. 1(a)]: first, the mean free time, τ_F, defined as the average span between collisions, which at low densities is synonymous with the mean free path divided

*sglotzer@umich.edu

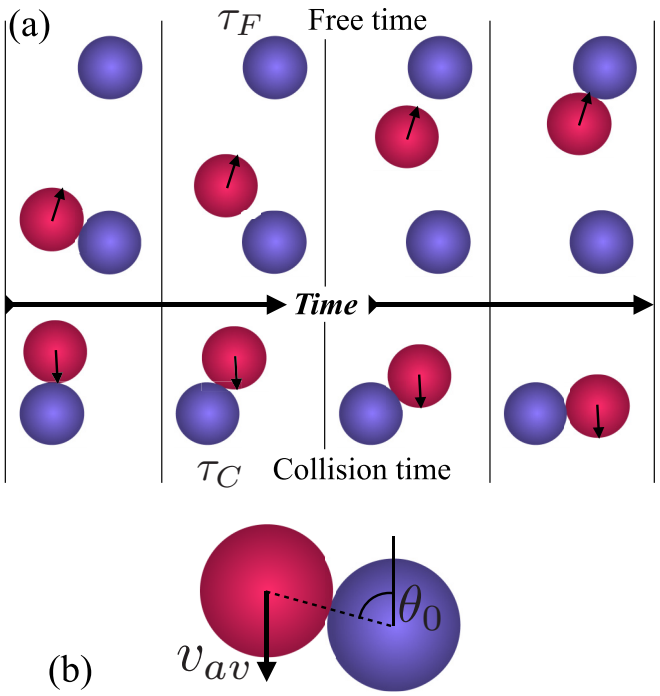

FIG. 1. (a) A schematic representation of two key timescales involved in the triggering of phase separation for active self-propelled particles. For a single active particle (red), the free time τ_F considers the time a particle spends between collision events, while the collision time τ_C considers the lifetime of a collision. (b) A schematic representation of the incident angle of collision θ_0, for Eq. (2).

by the particle's speed; and second, the mean collision time, τ_C, defined as the average lifetime of a two-particle collision. We propose that at the density where $\tau_C \gtrsim \tau_F$, which we call the *congestion density*, $\phi_{\rm con}$, particles experience a rate of collisions, τ_F^{-1}, that outpaces their rate of separating from a collision, τ_C^{-1}. This imbalance results in a positive feedback effect of particle congestion, which drives the formation of ABP clusters. Thus $\phi_{\rm con}$ sets a strict lower bound on the value of $\phi_{\rm crit}$ required for spinodal phase separation.

Both of these timescales can be calculated for ballistic ABPs, which we will later compare to simulation results. First, the mean free time, τ_F, can be determined from collision theory [37]. Beginning with two dimensions, we know that N particles, traveling with a speed v_0 at low densities, will each collide once on average by the time they have moved through an area equal to the averaged area available to them. This area is simply the total area divided by N, or $\frac{\pi\sigma^2}{4\phi}$, where σ is the particles' diameter, and ϕ is the area fraction of particles. The area swept out by an ABP is $2\sigma v_{\rm av}\tau_F$, where $v_{\rm av} = \frac{1}{\pi}\int_0^\pi \sqrt{2-2\cos\theta}\,d\theta = 4v_0/\pi$ is the relative velocity of an active particle compared to all other particles, averaged over all possible relative angles θ [37]. Likewise for three dimensions, the *available volume* is $\frac{\pi\sigma^3}{6\phi}$, while the *swept volume* is $\pi\sigma^2 v_{\rm av}\tau_F$, with $v_{\rm av} = \frac{1}{4\pi}\int_0^{2\pi}\int_0^\pi \sin\theta\sqrt{2-2\cos\theta}\,d\theta\,d\psi = 4v_0/3$. Setting these two areas (or volumes in three dimensions) equal to each other, the resulting mean free time for a particle to wait between collisions is

$$\tau_F = \frac{\pi^2\sigma}{32v_0\phi} \quad \text{(2D)},$$
$$\tau_F = \frac{\sigma}{8v_0\phi}. \quad \text{(3D)}. \tag{1}$$

To solve for the mean collision time τ_C, we consider on average how long two frictionless ABPs remain in contact when colliding. We frame a collision event such that one particle is held fixed and the other is moving downward with a velocity $v_{\rm av}$, and colliding at an incident angle θ_0, as shown in Fig. 1(b). In this instance, the incident angle-dependent collision time $\tau_{\rm inc}$ is simply the time it takes the ABP to move around its fixed neighbor and sweep out the angle between θ_0 and $\pi/2$,

$$\tau_{\rm inc}(\theta_0) = \int_{\theta_0}^{\pi/2} \frac{\sigma\,d\theta}{(1-\phi^*)v_{\rm av}\sin\theta}. \tag{2}$$

The correction to the velocity, $(1-\phi^*)$, linearly interpolates between the ideal unhindered movement of two isolated particles and the fully arrested state of particles found at a limiting density ϕ^*. Such a phenomenological factor has been measured directly in systems of active Brownian particles, and it is predicted from various kinetic theories [15,27,28,30]. Our application of this first-order correction to the collision velocity can be attributed to multibody collisions that act to hinder particle movement, and it gives τ_C its necessary density dependence. Although this linear relationship becomes inaccurate at higher densities, simulations show that it holds for $\phi \lesssim 0.5$ [28], which includes both the density ranges where $\tau_C \approx \tau_F$, and where phase separation occurs. Averaging over all possible incident angles θ_0 in both two and three dimensions yields

$$\tau_C = \frac{G}{1-\phi/\phi^*_{\rm 2D}} \quad \text{(2D)},$$
$$\tau_C = \frac{\ln(8)}{4(1-\phi/\phi^*_{\rm 3D})} \quad \text{(3D)}, \tag{3}$$

where $G \approx 0.916$ is Catalan's constant, and we assume movement becomes fully arrested at the area fraction of hexagonally packed disks in two dimensions, $\phi^*_{\rm 2D} \approx 0.907$, and the volume fraction of hexagonally close-packed spheres in three dimensions, $\phi^*_{\rm 3D} \approx 0.740$ [38]. (Previous studies estimate these densities using numerical fitting methods, which result in larger values of $\phi^*_{\rm 2D} \approx \phi^*_{\rm 3D} = 0.95$ [15,27].) Both τ_F and τ_C are plotted with respect to the average area fraction (or volume fraction in three dimensions), ϕ, as solid lines in Fig. 2. Adapting this calculation to various experimental active systems may require corrections that account for hydrodynamic effects, friction, and multibody collisions at larger densities; however, this simple first-order approximation is sufficient for an initial estimate of $\phi_{\rm con}$. Solving for the critical density for MIPS when $\tau_C = \tau_F$ yields $\phi_{\rm con} = 0.25$ for two dimensions and $\phi_{\rm con} = 0.18$ for three dimensions. We predict that for densities above $\phi_{\rm con}$, ABPs will experience on average a higher rate of new collisions compared to terminating collisions, thus resulting in a pileup of ABPs and phase separation.

To verify these values and to explicitly determine both $\phi_{\rm con}$ and $\phi_{\rm crit}$, we perform active particle dynamics simulations that

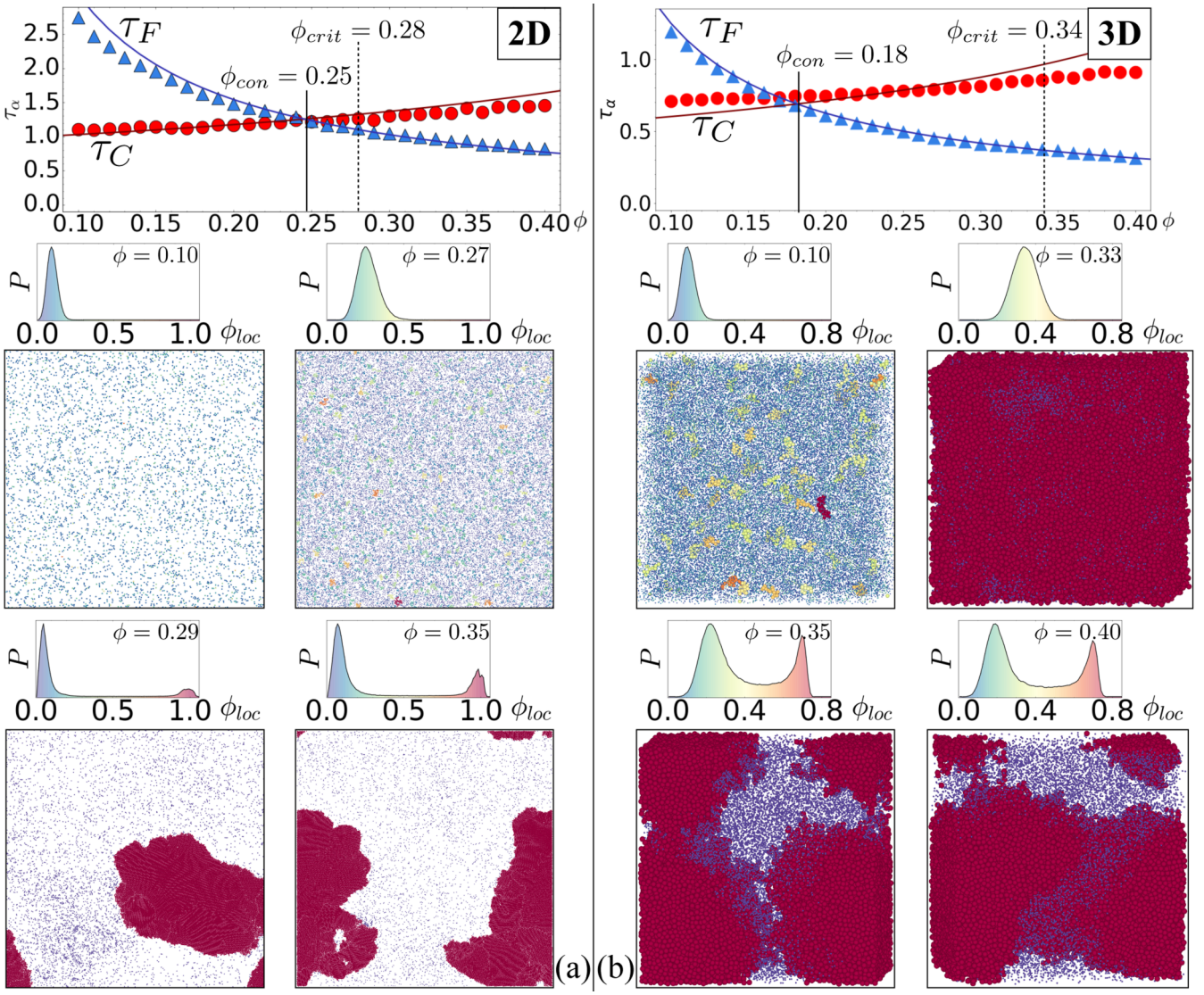

FIG. 2. The mean free time τ_F (blue triangles) and the mean collision time τ_C (red circles), as a function of area fraction ϕ, in both two (a) and three dimensions (b). Solid colored lines represent the predicted values calculated with Eqs. (1) and (3). The congestion density, being the minimum density required for phase separation, is the point where $\tau_C > \tau_F$ is $\phi_{\rm con} > 0.25$ for two dimensions and $\phi_{\rm con} > 0.18$ for three dimensions (marked with vertical solid lines). The critical density for phase separation found using simulations is $\phi_{\rm crit}$ (marked with the vertical dashed lines). Visualizations of the results at various densities are shown with particles colored by their cluster size. Local density histograms are also provided (using the same color scale), showing a transition from unimodal to bimodal distributions upon phase separation. For the 3D visualization, particles not belonging to a large cluster are reduced in diameter for easier viewing.

obey the Brownian equations of motion,

$$\gamma \dot{\mathbf{r}}_i = \mathbf{F}_i^{\rm SP} + \sum_j \mathbf{F}_{ij}^{Ex}, \qquad \dot{\theta}_i = \sqrt{2D_R}\eta_i, \tag{4}$$

where γ is the drag coefficient and η_i is Gaussian white noise, with $\langle \eta_i(t) \rangle = 0$, and $\langle \eta_i(t)\eta_j(t') \rangle = \delta_{ij}\delta(t-t')$ [39]. Each ABP experiences a self-propulsion force $\mathbf{F}_i^{\rm SP} = v_0\hat{n}_i = v_0(\cos\theta_i, \sin\theta_i)$ that undergoes rotational diffusion scaled by D_R. Nearby ABPs interact via a frictionless excluded-volume repulsive force $\mathbf{F}_{ij}^{Ex}$, given by the steeply repulsive Weeks-Chandler-Andersen potential (i.e., just the repulsive portion of the Lennard-Jones potential), with the particle diameter σ, defined as the distance where $\mathbf{F}_{ij}^{Ex} = 0$ [40]. The persistence length of the self-propulsion path is held constant at $\ell_P = 1000\sigma$. This value is chosen because ℓ_P/v_0 is several orders of magnitude greater than the timescales of τ_C and τ_F, and therefore it should not effect the onset of MIPS. To corroborate this assumption, previous studies have already reported a $\phi_{\rm crit}$ that is independent of ℓ_P for $\ell_P \gtrsim 100\sigma$ [28,30,31]. Time is measured in units of $\tau = \sigma/v_0$. The area fraction covered by N particles is $\phi = \frac{N\pi\sigma^2}{4A_{\rm tot}}$ in two dimensions and $\phi = \frac{N\pi\sigma^3}{6V_{\rm tot}}$ in three dimensions. All simulations were performed using the particle simulation toolkit, HOOMD-BLUE (version 2.1) [41], with a step size of $10^{-4}\tau$.

Simulations used to measure τ_F and τ_C were performed for $N = 2000$ particles in both two and three dimensions. Measurements were taken before steady state was reached by averaging over only the first 30τ of the simulations. This

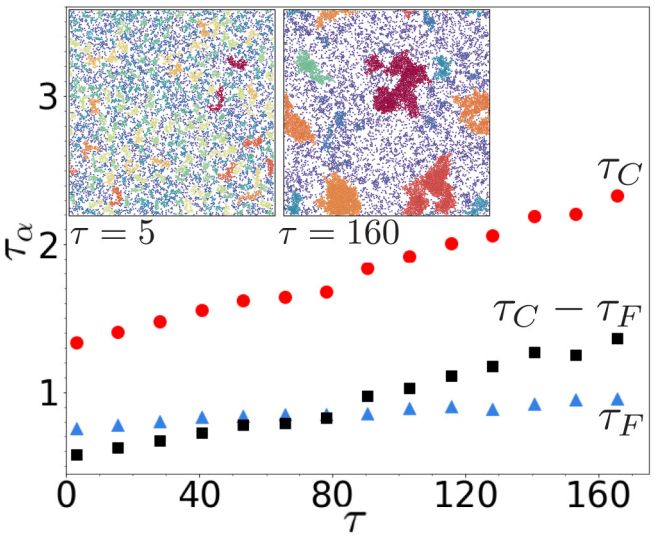

FIG. 3. Timescales τ_C (solid red line), τ_F (solid blue line), and $\tau_C - \tau_F$ (dashed black line), as a function of time τ in two dimensions. The density is $\phi = 0.4$, well above the spinodal of phase separation at $\phi_{\text{crit}} = 0.28$. Insets show snapshots at two different times, with particles colored by their cluster size. Each data point is averaged over at least 10 000 measurements.

choice permits a close comparison to the ideal-gas regime of the analytical results of Eqs. (1) and (3). Additionally, a system comprised of only 2000 particles still guarantees that ABPs have sampled only a fraction of the periodic simulation box, negating the typical requirement of $N \gtrsim 10\,000$ necessary to ignore finite number effects that have been observed in previous studies [33]. The initial state was generated by placing particles at random locations and then relaxing their positions via a repulsive spring force to remove all particle overlaps. The direction of the self-propulsion force for each particle, $\hat{n}_i$, was also assigned randomly. This initial state approximates equilibrated passive particles that then have their self-propulsion activated. The specific procedure to generate the initial random state was found to have little effect on the measurements of τ_C and τ_F.

τ_F is calculated as the mean duration that particles spend completely free of contact (defined as $\mathbf{F}_{ij}^{Ex} = 0$), while τ_C is calculated as the mean duration of any two-particle contacts. Evidently, the accessible timescales of the initial state are sufficient to determine the final steady-state behavior. The short 30τ period of time is sufficient to measure the desired timescales well before phase separation. This is true even in the worst-case scenario when the density is well above ϕ_{crit}, where clusters quickly begin to nucleate and grow, thus greatly changing τ_C and τ_F. To demonstrate this point, Fig. 3 shows steadily increasing collision and free timescales for $\phi = 0.4$. By 30τ, both timescales have increased by less than 10%. The increase of τ_C with time is explained by ABPs becoming trapped in ever-growing clusters, which can be seen in the inset visualizations at $\tau = 5$ versus $\tau = 160$. Meanwhile, τ_F also increases with time because there are fewer particles in the dilute phase, thus increasing the mean free path of active particles that are not yet trapped in clusters. Most importantly, however, the difference between the two timescales, $\tau_C - \tau_F$, also grows with time, which acts to further increase the drive for phase separation. Eventually, the phase-separated steady state is reached (after $\sim 10^5\tau$), resulting in plateaued values of τ_C and τ_F with time. In other words, a system undergoing phase separation enters a positive feedback loop where clustering decelerates particles, which locally increases the lifetime of collisions τ_C, which leads to growing clusters, which decelerates more particles, and so on. Alternatively, for densities below ϕ_{crit}, clusters remain relatively small and short-lived, effecting little change in τ_C and τ_F beyond what is measured over the first 30τ. Overall, this behavior confirms that the density ϕ_{con} at which $\tau_C > \tau_F$ is a necessary lower bound for ϕ_{crit}. In the end, we are able to obtain accurate statistics using only the first 30τ of an initially random system.

Measurements for τ_C and τ_F under these simulation parameters for both two and three dimensions are shown in Fig. 2. The results fit well with the analytical solutions of Eqs. (1) and (3), even up to $\phi = 0.4$. This density regime is well beyond where the assumptions of low density are expected to hold, namely that only uninterrupted two-body collisions are present (assumed when approximating τ_C), and, more surprisingly, that all collisions can be ignored and our system behaves like an ideal gas (assumed when approximating τ_F).

Now that τ_C and τ_F are established, we show that the inequality $\tau_C > \tau_F$ is indeed a minimal requirement for MIPS of ABPs. To determine the ϕ_{crit} at which this happens, we perform full simulations of $N = 50\,000$ particles for $4 \times 10^7\tau$. This ensures measurements are made after reaching the final steady-state behavior, and that finite number (and finite persistence length) effects can be ignored. The measurements for ϕ_{crit} are marked as the vertical dashed lines in Fig. 2. Phase separation is observed at $\phi_{\text{crit}} \approx 0.28$ for two dimensions and $\phi_{\text{crit}} \approx 0.34$ for three dimensions, determined by the development of a bimodal distribution in the local density histogram [14]. Example histograms, along with visualizations of the systems at four values of ϕ, both near and far from the transition, are provided in Fig. 2. Both two-dimensional (2D) and three-dimensional (3D) measurements of ϕ_{crit} are above the minimum values of ϕ_{con} predicted from both Eqs. (1) and (3).

The reason $\phi_{\text{crit}} \geqslant \phi_{\text{con}}$ is because ϕ_{con} sets the minimum density required for two-particle clusters to, on average, live long enough to grow. However, this behavior is not sufficient to attain full phase separation at ϕ_{crit}. This is because ϕ_{con} assumes only ideal two-particle collisions at low density; but in reality, the formation of the dense phase requires many multiparticle collisions. Therefore, one must consider the lifetimes of these multiparticle clusters to determine if they themselves grow into a larger phase-separated cluster or disperse back into the dilute phase. To quantify this behavior, if τ_C and τ_F measure the average timescales experienced by a single particle, we define similar quantities for a dense cluster consisting of n particles, where the corresponding rates are not simple linear functions of n. Specifically, one can argue that the average time between particles leaving a cluster of size n is $\tau_C^{(n)} \gtrsim \tau_C/n$, because multiparticle clusters can cooperatively act to stabilize a collision and increase its lifetime; and similarly, the average time between particles adding to a cluster is $\tau_F^{(n)} \gtrsim \tau_F/n$, because the collision cross section of a cluster is on average less

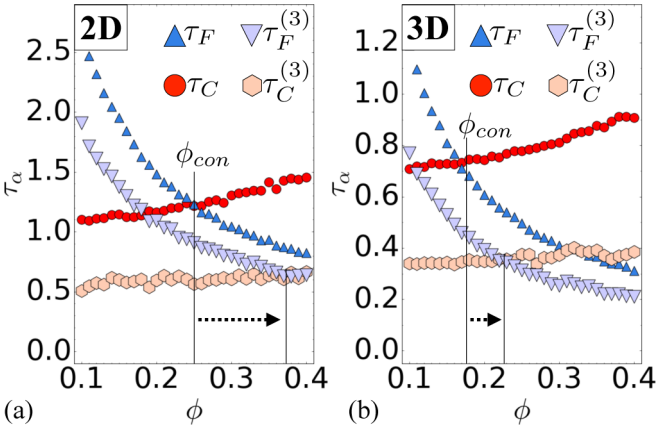

FIG. 4. Average timescale measurements from simulations for clusters consisting of $n = 3$ particles in both (a) two dimensions and (b) three dimensions. The average individual timescales for all particles from Fig. 2 are also shown for comparison. Larger clusters tend to have a crossover of $\tau_C^{(n)} = \tau_F^{(n)}$ at a density higher than $\tau_C = \tau_F$ (marked with vertical lines).

than $n2\sigma$ (or $n\pi\sigma^2$ in three dimensions). Values for $\tau_C^{(3)} = \tau_F^{(3)}$, measured in simulations for clusters of size $n = 3$, are shown in Fig. 4; these values verify the above inequalities. The end result is that $\phi_{\rm con}$, which is set by when $\tau_C = \tau_F$, is not sufficient alone to determine $\phi_{\rm crit}$; nevertheless, this timescale analysis does yield an accurate lower bound density for MIPS.

Furthermore, these multiparticle collisions explain why the inequality of $\phi_{\rm crit} \geqslant \phi_{\rm con}$ is greater in three dimensions than two dimensions, as is obvious in Fig. 2. This behavior can be largely attributed to the fact that the extra third dimension provides an additional direction for particles to slide past each other. Whereas in two dimensions, two particles in contact occupy 1/6th of their available solid angle, in three dimensions this decreases to $< 1/13$th [38]. Therefore, 3D particles are much less likely to pile up into multiparticle clusters with many contacts, and consequently have a much smaller $\tau_C^{(n)}$ than 2D particles for all values of n. This results in 3D multiparticle clusters that are too short-lived to induce phase separation, which is only overcome at densities well above $\phi_{\rm con}$.

In conclusion, by comparing the timescales associated with collisions of ABPs, we have determined a lower bound on the critical density, $\phi_{\rm crit}$, required for MIPS. Our findings provide microscopic insight into the mechanism of early-stage MIPS, and they supplement the existing kinetic and continuum-based theories by describing the behavior of ABPs in the ballistic regime. This theory uniquely describes the ballistic regime of $\ell_P/\sigma \to \infty$, where a strict notion of global ergodicity is lost; however, ergodicity persists on the small size and time scales relevant to early stage phase separation, which allows for the determination of a system's average behavior. Importantly, we determine that, at minimum, phase separation requires a density high enough to achieve congestion, where the mean lifetime of a collision, τ_C, is larger than the mean time between collisions, τ_F. Surprisingly, a simple ideal gas regime calculation—resulting in Eqs. (1) and (3)—is sufficient to calculate $\phi_{\rm con}$, which in turn sets a lower bound for $\phi_{\rm crit}$.

From this foundation, one can now account for the rotational noise of ABPs and allow τ_C and τ_F to be functions of ℓ_P. Interestingly, as long as $\ell_P \gtrsim \sigma$, this results in $\tau_F(\ell_P)$ being equal to the τ_F from Eq. (1), because the path of an active particle still remains relatively straight in this regime. Similarly, when $\ell_P \gtrsim \sigma$, $\tau_C(\ell_P)$ remains relatively unchanged from Eq. (3), because the timescale of rotational diffusion, D_R^{-1}, is insignificant when larger than the average lifetime of a two-particle collision. A full analysis, both numerical and analytical, concludes with a predicted $\phi_{\rm con}$ that increases only when $\ell_P \lesssim \sigma$. This outcome clearly fails to account for the observed increase in $\phi_{\rm crit}(\ell_P)$ for as early as $\ell_P \lesssim 100\sigma$ [28,30,31]. In this regime, our claims of a lower bound on $\phi_{\rm crit}$ set by $\tau_C(\ell_P) > \tau_F(\ell_P)$ still hold true; however, there emerges a new ℓ_P-dependent length scale that accounts for the rate of particles escaping a cluster into the dilute phase. These events act to further regulate large-scale phase separation by increasing $\phi_{\rm crit}$ with decreasing ℓ_P [14,26].

Beyond rotational noise, there are a variety of additional considerations that can affect $\phi_{\rm con}$, and therefore $\phi_{\rm crit}$. These include (i) the role of particle shape, which may act to increase τ_C, and thus $\phi_{\rm crit}$, if facets are present [19,20], or alternatively to decrease $\phi_{\rm crit}$ by increasing τ_F in the case of active rods that have a tendency to swarm [16–18]; (ii) the role of passive particles mixed with ABPs, which increases $\phi_{\rm crit}$ by perhaps increasing the effective τ_F [24,25]; (iii) the influence of fixed barriers, which decrease $\phi_{\rm crit}$, conceivably by trapping particles and greatly increasing τ_C [42,43]; (iv) the role of interparticle attraction, which would lower $\phi_{\rm crit}$ through a simultaneous increase of τ_C and decrease of τ_F [21]; (v) the role of particle elasticity, which could see an increase in $\phi_{\rm crit}$ for "softer" particles through a lowering of τ_C, as suggested by an increased $\phi_{\rm crit} = 0.46$ found for ballistic active particles with soft harmonic repulsion [43]; (vi) the role of particle "eccentricity" (i.e., orbiting ABPs with an off-centered self-propulsion force), which can lose their ability to phase-separate, possibly because rotating particles can easily slide past each other and lower their τ_C [44]; (vii) the complex role of hydrodynamics, which may result in either enhanced or diminished phase separation depending on if the particles are "pushers" versus "pullers," and/or if they are fully 3D versus confined quasi-2D [45–48]; (viii) or the role of non-negligible particle inertia [49]. These examples demonstrate that the multitude of active matter systems beyond the *vanilla* ABP model possess a rich behavior that could possibly be understood in terms of congestion on the microscopic scale. However, a full quantitative exploration of τ_C and τ_F in each variant is left as an open question.

We thank Shannon Moran and Mayank Agrawal for helpful feedback, and Michael Hagan and Michael Cates for insightful discussions. This work was supported as part of the Center for Bio-Inspired Energy Science, an Energy Frontier Research Center funded by the U.S. Department of Energy, Office of Science, Basic Energy Sciences under Award No. DE-SC0000989. Computational resources and services were supported by Advanced Research Computing at the University of Michigan, Ann Arbor.

[1] M. C. Marchetti, J. F. Joanny, S. Ramaswamy, T. B. Liverpool, J. Prost, M. Rao, and R. A. Simha, Rev. Mod. Phys. **85**, 1143 (2013).

[2] S. Ramaswamy, Annu. Rev. Condens. Matter Phys. **1**, 323 (2010).

[3] J. Palacci, S. Sacanna, A. P. Steinberg, D. J. Pine, and P. M. Chaikin, Science **339**, 936 (2013).

[4] J. Palacci, S. Sacanna, S. Kim, G. Yi, D. J. Pine, and P. M. Chaikin, Philos. Trans. R. Soc. London, Ser. A **372**, 20130372 (2015).

[5] G. Volpe, I. Buttinoni, and D. Vogt, Soft Matter **7**, 8810 (2011).

[6] V. Narayan, S. Ramaswamy, and N. Menon, Science **317**, 105 (2007).

[7] J. Deseigne, O. Dauchot, and H. Chaté, Phys. Rev. Lett. **105**, 098001 (2010).

[8] H.-R. Jiang, N. Yoshinaga, and M. Sano, Phys. Rev. Lett. **105**, 268302 (2010).

[9] A. Snezhko and I. S. Aranson, Nat. Mater. **10**, 698 (2011).

[10] A. Snezhko, M. Belkin, I. S. Aranson, and W. K. Kwok, Phys. Rev. Lett. **102**, 118103 (2009).

[11] É. Fodor, C. Nardini, M. E. Cates, J. Tailleur, P. Visco, and F. van Wijland, Phys. Rev. Lett. **117**, 038103 (2016).

[12] M. E. Cates and J. Tailleur, Europhys. Lett. **101**, 20010 (2013).

[13] Y. Fily and M. C. Marchetti, Phys. Rev. Lett. **108**, 235702 (2012).

[14] G. S. Redner, M. F. Hagan, and A. Baskaran, Phys. Rev. Lett. **110**, 055701 (2013).

[15] J. Stenhammar, D. Marenduzzo, R. J. Allen, and M. E. Cates, Soft Matter **10**, 1489 (2014).

[16] H. H. Wensink and H. Löwen, J. Phys.: Condens. Matter **24**, 464130 (2012).

[17] M. Abkenar, K. Marx, T. Auth, and G. Gompper, Phys. Rev. E **88**, 062314 (2013).

[18] S. Mishra, J. Stat. Mech.: Theor. Exp. (2014) P07013.

[19] H. H. Wensink, V. Kantsler, R. E. Goldstein, and J. Dunkel, Phys. Rev. E **89**, 010302(R) (2014).

[20] S. E. Ilse, C. Holm, J. D. Graaf, S. E. Ilse, C. Holm, and J. D. Graaf, J. Chem. Phys. **145**, 134904 (2016).

[21] G. S. Redner, A. Baskaran, and M. F. Hagan, Phys. Rev. E **88**, 012305 (2013).

[22] V. Prymidis, H. Sielcken, and L. Filion, Soft Matter **11**, 4158 (2015).

[23] M. Agrawal, I. R. Bruss, and S. C. Glotzer, Soft Matter **13**, 6332 (2017).

[24] J. Stenhammar, R. Wittkowski, D. Marenduzzo, and M. E. Cates, Phys. Rev. Lett. **114**, 018301 (2015).

[25] A. Wysocki, R. G. Winkler, G. Gompper, N. Podewitz, F. Jülicher, G. Gompper, A. Wysocki, R. G. Winkler, and G. Gompper, New J. Phys. **18**, 123030 (2016).

[26] G. S. Redner, C. G. Wagner, A. Baskaran, and M. F. Hagan, Phys. Rev. Lett. **117**, 148002 (2016).

[27] J. Stenhammar, A. Tiribocchi, R. J. Allen, D. Marenduzzo, and M. E. Cates, Phys. Rev. Lett. **111**, 145702 (2013).

[28] M. E. Cates and J. Tailleur, Annu. Rev. Condens. Matter Phys. **6**, 219 (2015).

[29] C. Nardini, É. Fodor, E. Tjhung, F. van Wijland, J. Tailleur, and M. E. Cates, Phys. Rev. X **7**, 021007 (2017).

[30] Y. Fily, S. Henkes, and M. C. Marchetti, Soft Matter **10**, 2132 (2014).

[31] A. P. Solon, J. Stenhammar, M. E. Cates, Y. Kafri, and J. Tailleur, Phys. Rev. E **97**, 020602 (2018).

[32] D. Levis, J. Codina, and I. Pagonabarraga, Soft Matter **13**, 8113 (2017).

[33] I. R. Bruss and S. C. Glotzer, Soft Matter **13**, 5117 (2017).

[34] J. Tailleur and M. E. Cates, Phys. Rev. Lett. **100**, 218103 (2008).

[35] D. Aswad and D. E. Koshland Jr., J. Bacteriol. **118**, 640 (1974).

[36] M. Molaei, M. Barry, R. Stocker, and J. Sheng, Phys. Rev. Lett. **113**, 068103 (2014).

[37] M. J. Pilling and P. W. Seakins, *Reaction Kinetics* (Oxford University Press, Oxford, 1995).

[38] D. Weaire and T. Aste, *The Pursuit of Perfect Packing, Second Edition* (CRC, Boca Raton, FL, 2008).

[39] S. Henkes, Y. Fily, and M. C. Marchetti, Phys. Rev. E **84**, 040301 (2011).

[40] H. C. Andersen, J. D. Weeks, and D. Chandler, J. Chem. Phys. **54**, 5237 (1971).

[41] J. A. Anderson, C. D. Lorenz, and A. Travesset, J. Comput. Phys. **227**, 5342 (2008).

[42] A. Kaiser, H. H. Wensink, and H. Löwen, Phys. Rev. Lett. **108**, 268307 (2012).

[43] C. Reichhardt and C. J. Olson Reichhardt, Soft Matter **10**, 7502 (2014).

[44] Z. Ma, Q.-L. Lei, and R. Ni, Soft Matter **13**, 8940 (2017).

[45] A. Zöttl and H. Stark, Phys. Rev. Lett. **112**, 118101 (2014).

[46] R. Matas-Navarro, R. Golestanian, T. B. Liverpool, and S. M. Fielding, Phys. Rev. E **90**, 032304 (2014).

[47] J. Blaschke, M. Maurer, K. Menon, A. Zöttl, and H. Stark, Soft Matter **12**, 9821 (2016).

[48] N. Oyama, J. J. Molina, and R. Yamamoto, Phys. Rev. E **93**, 043114 (2016).

[49] R. Golestanian, Phys. Rev. Lett. **102**, 188305 (2009).